

M.L. Burt · G. Wadge · R.N. Curnow

An objective method for mapping hazardous flow deposits from the stratigraphic record of stratovolcanoes: a case example from Montagne Pelée

Received: 4 January 2000 / Accepted: 5 January 2001 / Published online: 13 March 2001
© Springer-Verlag 2001

Abstract A method is described that enables a variety of maps, which indicate the probabilities of deposition, to be constructed in a reproducible manner from the stratigraphic information typically available at well-studied stratovolcanoes. These maps can then be used as a basis for hazard assessment. The sampling of the deposits of previous eruptions is subject to uncertainties due to erosion, sectoral deposition and non-exposure. A model-based, iterative algorithm is used to compensate for the incomplete sampling. For each site, the available evidence from the other sites is used to estimate the probability of deposition for missing deposits. A geographical information system (GIS)-based method that uses Thiessen polygons to represent the presence or absence of deposits, together with simple cartographic rules based on depositional processes, then defines the extent of deposition. The combined operation of these two techniques is presented for Montagne Pelée in Martinique, using the amended stratigraphic record of Smith and Roobol (1990) for the past 6000 years. Three types of maps are created: maps for individual depositional events (the 1902 block-and-ash flow and surge deposits are used to verify the technique); maps for different deposit types aggregated over 6000 years of activity; and scenario maps which, in Montagne Pelée's case, recognise that

during the next Peléean or Plinian eruption a variety of hazards will have to be confronted.

Keywords Volcanic hazards · Hazard maps · Eruption statistics · Explosive volcanism · Stratigraphic record

Introduction

The map has been, and is likely to continue to be, the prime medium for representing spatial information on volcanic hazards. In this paper we present new methods to construct maps of deposits from the stratigraphic record of a stratovolcano. These deposition maps can then be used as the basis of a hazard assessment. We apply our methods to Montagne Pelée, Martinique, West Indies.

In the absence of a detailed historical record of activity, an assessment of future hazards from a stratovolcano should be largely based on stratigraphy and past activity. In practice, many hazard maps of volcanoes contain little information from stratigraphic study (Rosi 1996). The stratigraphic record typically consists of sparse site observations of deposits from past eruptions. Moreover, stratigraphic sequences are often imperfectly dated (Harkness et al. 1994) and tend to be incomplete. We need to be aware of the limitations of the record and, if possible, compensate for it. We have used a model-based iterative algorithm to make the most of the information available from sites with an incomplete record of deposits.

Accurately predicting the areas affected by an explosive eruption is important. In many cases, areas thought to be hazardous tend to be defined either by simple geometric shapes or enclosed by subjectively drawn boundaries. Models based on the physics of volcanic processes are being developed (e.g. Woods 1998; Druitt 1998). Such models require a large number of parameters to be estimated and it is unlikely that values for all these parameters can be estimated accurately. We use an intermediate approach, with boundaries based on simplified

Editorial responsibility: S. Carey

M.L. Burt (✉) · G. Wadge
Environmental Systems Science Centre,
University of Reading, 3 Earley Gate,
Reading, RG6 6AL, UK
e-mail: louise@mcs.st-andrews.ac.uk
Fax: +44-1334-463748

R.N. Curnow
Department of Applied Statistics, University of Reading,
Harry Pitt Building, Whiteknights Road, PO Box 240,
Reading, RG6 6FN, UK

Present address:

M.L. Burt, Research Unit for Wildlife Population Assessment,
Mathematical Institute, North Haugh, University of St. Andrews,
St. Andrews, KY16 9SS, UK

physical models of the processes. The boundary models developed in this paper are used to delineate between areas of deposition and non-deposition from pyroclastic flows and surges. We combine these models with the probability of deposition to create a variety of maps. The maps could be used to predict the hazard, e.g. from flow phenomena that affect greater areas than those affected by deposition, although we do not consider these hazards herein. The mapping of airfall deposits and lava flows are also not considered. Objective methods for predicting lava flow and airfall hazards have been described by Wadge et al (1994) and Barberi et al (1990), respectively.

The stratigraphy of Montagne Pelée has been well studied, notably by Westercamp and Traineau (1983), and Smith and Roobol (1990). Smith and Roobol (1990) included information on deposits from 30 stratigraphic sections. All the major processes displayed by a stratovolcano, except major structural collapse, have been identified and are likely to threaten the inhabitants of Martinique in a future eruption. Maps of deposit distribution from past events have also been published (Westercamp and Traineau 1983; Traineau et al. 1989; Smith and Roobol 1990) and we use these for comparison.

This paper is divided into four main sections. Firstly, we consider a stratigraphic record from a typical stratovolcano, which tends to be incomplete in time and space. We describe methods for improving the information contained in the stratigraphic record by (a) estimating the probability of deposition at a site where a deposit is missing, based on the information at other sites, and (b) creating maps of deposits using cartographic models of eruptive processes. Finally, we combine these techniques in Application to Montagne Pelée (see later).

Stratigraphic record of a stratovolcano

Ideally, the stratigraphy of the volcano should be based on knowledge of the complete areal extent and thickness of all deposits. In reality, the rocks are usually only exposed in cliffs or quarry faces and so often the stratigraphy is based on several vertical sections scattered around the volcano. The observed stratigraphic record is essentially a sampling in space and time of the true deposits and is, in most cases, incomplete in both.

Incomplete spatial sampling

Stratovolcanoes with a central vent generally have the shape of a truncated cone with concave-upward slopes. The cone consists of deposits that can be thought of as distinct elements with sectoral boundaries (Fig. 1a). Elements can extend beyond the sampling space, e.g. much of the volcanic production from island volcanoes are deposited in the sea (Sigurdsson et al. 1980). Each stratigraphic section typically consists of numerous records

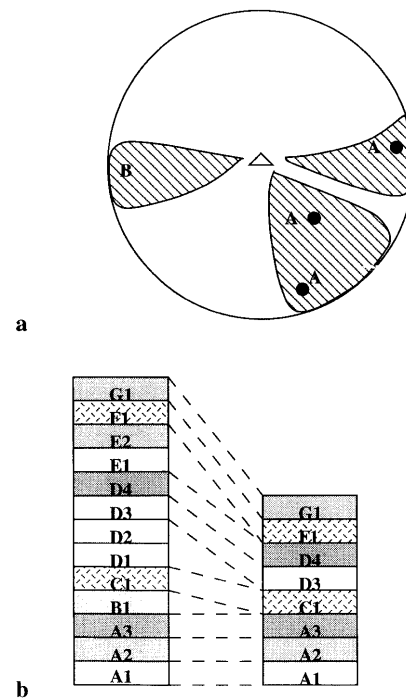


Fig. 1a, b Oversampling and undersampling of deposits on a stratovolcano. **a** Deposits, denoted by the shaded areas on the map, can be missed in a sparse sampling scheme. Deposit A has been sampled at the stratigraphic sites marked by a dot. Deposit B has not been sampled. **b** Individual eruptive periods may be over-sampled and undersampled in the preserved stratigraphic sequence (right column). The complete stratigraphic record is on the left. Letters denote deposits from the same eruptive period. Numbers refer to separate deposits from an individual eruptive period. Deposits may be of different types, indicated by shading

relating to distinct elements. These records tend to be incomplete because: (a) the areal distribution of the samples tends to be sparse and does not cover the whole sampling space; (b) some depositional elements are sectoral and hence may be missed if the sampling scheme is sparse; (c) some elements have been removed by erosion; and (d) areas affected by flow phenomena can be greater than areas of deposition.

Incomplete temporal sampling

The stratigraphic record may over-sample individual eruptive periods that produce multiple deposits and under-sample the full eruptive record because deposits have been eroded. For example, in Fig. 1b the complete eruption record is ABCDEFG, where each letter represents an eruption and the numbers individual layers. The apparent eruption record reconstructed from the observed stratigraphic record would be AAACDDFG. Erosion causes the partial or complete removal of eruptive products and may leave an obvious erosional unconformity. Deposits from small eruptions are eroded more readily than more voluminous deposits; hence, for older eruptions, there is a bias towards larger events

with smaller events being missed altogether. This bias is less for more recent eruptions which have suffered less erosion. Also, the older the eruption, the less likely it is to be exposed because of how deep the section would have to extend. The further the record extends back in time, the less complete it becomes. Reconstructing volcanic stratigraphy is further complicated by non-deposition and unconformities. Non-deposition occurs if products of a volcanic eruption are restricted to a narrow sector on one side of the volcano or confined to certain valleys. It is therefore more likely that these deposits will be missed in a sparse sampling scheme.

Estimating probabilities of deposition

It is necessary to consider the quality of the stratigraphic record, and the time interval that is to be used, in the hazard assessment. As explained later, this is an important consideration. A visual check of the depositional units plotted against time may be all that is necessary to decide on the completeness of the record. Part of the record thought to be greatly under-sampled could simply be ignored. Also, physical and chemical changes of the volcano may have modified the overall pattern of events; therefore, including the stratigraphy before this change may not be appropriate for an assessment of present hazards.

Stratigraphic record as a matrix

The stratigraphic record can be expressed in the form of a matrix, with the time units (depositional units) as rows and the spatial units (stratigraphic sites) as columns. Each depositional unit could be the product of an individual eruption, or one phase of an eruption, or a cluster of activity that cannot be separated because of uncertainties associated with dating. Assume that each eruptive event is represented at least at one of the sites; then the stratigraphy is a complete record of the eruptive history. The cells in the matrix, denoted by d_{it} , contain the probabilities of a deposit belonging to depositional unit t and occurring at site i . Where a deposit from a particular depositional unit has been identified at a site, the probability of deposition is unity (termed a definite presence). Where a deposit is absent, the probability is initially set to zero. If a deposit is present, but the exact unit attribution is unknown, then the probability of unity is divided among all possible depositional units for this deposit in a way that is described in Application to Montagne Pelée (see later). We call these depositional units constrained units. Some depositional units may be censored in that it is known only that they were deposited either before or after a known depositional unit. We call this matrix of known and inferred probabilities, d_{it} , the observed matrix of depositional probabilities.

The absence of a deposit at a given site may be due to several reasons:

1. The site was not affected.
2. The site was affected but there was no deposition there.
3. There was deposition but either the deposit has subsequently been eroded from the stratigraphic record or has not been recorded because of (a) misidentification, or (b) it is in an unavailable measuring interval (e.g. the deposit is below ground at that site).

If a deposit is absent because of item 1, then assigning a probability of zero is correct. If a deposit is missing because of item 2 or item 3, the “absent” label should be changed to “present” and hence the probability changed to one. Unfortunately, item 1 cannot be distinguished from item 2 or item 3.

We have devised an algorithm to address this uncertainty, and to estimate the probabilities of deposition in order to minimise incompleteness in the stratigraphic record. Of course, our assumption that the stratigraphy is complete is not, in many cases, valid, and so we are limited to estimating the probability of deposition relative to the observed deposits; however, our algorithm allows us to make the most of the available information.

Algorithm to estimate the probabilities of deposition

The algorithm is an iterative procedure that correlates deposit occurrences over all sites. The probability that a deposit, now missing, was once present is estimated using the information from other sites.

Let D be the matrix containing elements d_{it} , the probabilities of a deposit of unit t and site i where $t=1\dots T$ and $i=1\dots N$. The youngest depositional unit is $t=1$.

Also, let old be a vector containing the depositional unit of the oldest deposit for each site. The oldest deposit could either have a probability of one, or be the last depositional unit in a sequence in which the probabilities sum to one. Now for each pair of sites i and j ,

$$\text{if } old_i < old_j, \text{ then let } l_{ij} = old_i, \text{ or else } l_{ij} = old_j. \quad (1)$$

Thus, L is a matrix with each element, l_{ij} , marking the youngest deposit out of the two oldest deposits for the pair of sites i and j . Probabilities of a deposit at site i given a deposit at site j are then calculated using only the deposits at sites i and j that are l_{ij} and younger. Ignoring deposits older than l_{ij} means that weight is only given to more recent deposits and where there is information at both sites. A zero probability assigned to an absent deposit is more likely to be zero for younger deposits, i.e. they are zero because of non-deposition rather than erosion. Also, if the information below the oldest dated depositional unit in each section cannot be relied on – if, for example, only the top of the section is visible – then older deposits will be assigned a probability of zero when, in fact, the information is unavailable.

The frequency of a deposit at site i , given that there is a deposit at site j , is used to obtain an estimate, pd_{ij} , of the probability of a deposit at site i given one at site j at any time in the record. It is assumed that the conditional probability that a deposit is missing is constant over time. This assumption may be doubtful, except over short periods, but this problem can be alleviated by considering only that part of the record thought to be the most complete and of similar quality. Hence, by probability calculations

$$pd_{ij} = \frac{\sum_{t=1}^{l_{ij}} d_{it}d_{jt}}{\sum_{t=1}^{l_{ij}} d_{jt}}. \quad (2)$$

Similarly, an estimate, pn_{ij} , of the probability of a deposit at site i given that there has been no deposit at site j is

$$pn_{ij} = \frac{\sum_{t=1}^{l_{ij}} d_{it}(1-d_{jt})}{\sum_{t=1}^{l_{ij}} (1-d_{jt})}. \quad (3)$$

Then the elements, ud_{it} , of a matrix D_1 , the “updated” probability of a deposit at site i and depositional unit t , are calculated by combining pd_{ij} and pn_{ij} using the original D matrix. For each d_{it} not equal to one

$$ud_{it} = \frac{\sum_{j=1}^N [pd_{ij}d_{jt} + pn_{ij}(1-d_{jt})]}{(N-1)} i \neq j. \quad (4)$$

We now take the updated D_1 as our matrix in place of D and iterate again to form a new matrix D_2 and so on until the sequence of matrices converges. The sequence is said to have converged when the maximum difference between any corresponding elements in the two updated matrices is less than a given tolerance. The final matrix is termed the estimated matrix of depositional probabilities. Those cells originally containing unity, i.e. a definite presence, are not changed, but the probabilities assigned to constrained and censored depositional units are changed according to the deposition at other sites. The probabilities that summed to one over several depositional units in the original matrix are also summed to one after applying the algorithm.

The algorithm estimates the probability that a deposit was once present, based on the presence of deposits at other sites and the similarity of other deposits between sites. Spatial information about the sites is not taken into account, although it may be useful to do so. One way to incorporate this would be to include a distance measure so that more weight is given to the information from sites located close together. This idea underlies the geostatistical technique called kriging. This approach may be appropriate for deposits likely to cover wide areas, such as laterally directed blasts, but it is not appropriate for deposits which are affected by topography. Using topography to define depositional boundaries is discussed in the following section.

A separate matrix is constructed for each deposit type. In all cases the algorithm can only estimate the complete record for sites that have a deposit of the type specified. Some sites may have had all traces of deposits removed; however, this problem is alleviated by the methods described below to map the pattern of occurrence of the deposits.

Mapping the extent of deposition

Selecting stratigraphic sites where a particular deposit has been identified is a means of representing whether the deposit is present or absent. This is essentially a map of points in a plane; however, a map showing the areal distribution of the presence/absence of a deposit is required.

One way of defining areas from points is to use a Thiessen polygon system. Thiessen polygons, also known as Voronoi diagrams or Dirichlet cells (Okabe et al. 1992), divide up a region in a way that is totally determined by the configuration of the sample points (Fig. 2a). All locations within the plane are associated

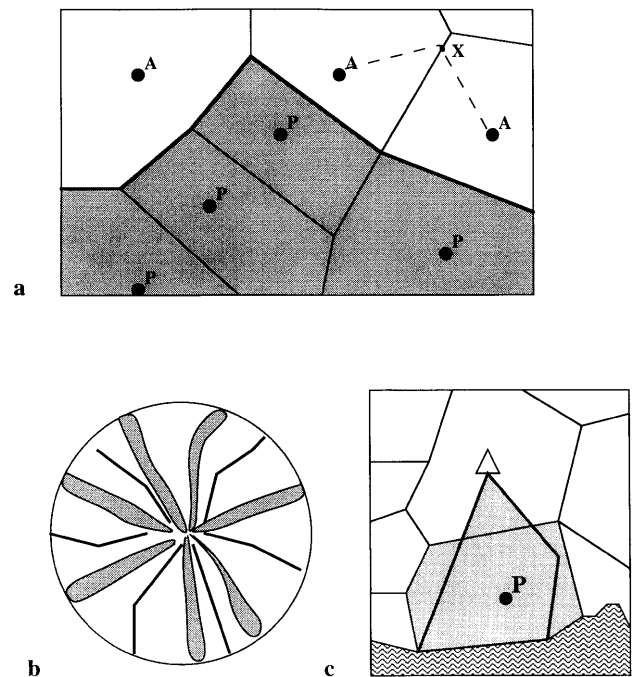


Fig. 2 a The Thiessen polygons generated for the system of stratigraphic sites indicated by dots. Point X is equidistant from two sites, shown by the dashed lines. A P indicates that the deposit is present at a site and so the deposit is assumed to have covered the whole of the polygon associated with that site. An A indicates that the deposit is absent. The bold line marks the deposit boundary between the polygons where the deposit is present and absent. b Schematic representation of watersheds and drainage channels. A plan view of topography assuming a circular base. The watersheds are shown in bold. Shaded regions represent narrow channels, which closely follow the rivers. c A combination of a Thiessen polygon and watershed–valley boundary represents the shaded area for this surge deposit. The vent is marked by a triangle, the sea by wavy hatching

with the closest point and the set of locations assigned to a particular point form a polygon. Some locations are equally close to two or more points, e.g. point X in Fig. 2a. The set of locations equally close to two or more points form the boundaries between adjacent regions. In the algorithm, we assume that where a deposit has been identified at a particular site, or point, then the whole polygon will have been covered by the deposit. Hence, the boundary of the deposit is the boundary between those polygons where the deposit is present or absent (Fig. 2a); thus, information about an unsampled location can be gained from information available at the closest sampled site to the unsampled site.

At a stratovolcano, a central vent, whose position is known, is usually the source of all pyroclastic deposits. We assume here that intercalated deposits from other volcanic centres can be identified and separated from the data set. There may be little or no information about deposits at, or close to, the vent because of accessibility problems; however, it is assumed that the area was affected. By considering the vent as a point, an area around the vent is generated in the Thiessen polygon system.

Whereas the Thiessen polygon system is a useful and objective mapping technique, knowledge of the processes involved in the formation of the deposits can be added to the technique to better constrain the location of the deposit boundaries. We make a simple division between flow processes that are influenced by the topography of the volcano and those that are not. The spatial distribution of these deposits are modelled in different ways.

Pyroclastic flows and lahars

Pyroclastic flows and lahars are driven by gravity and their flow paths are strongly influenced by topography (McEwan and Malin 1989); therefore, a simple method to map gravity-driven flows would be to use major valleys. For example, if a lahar deposit is located in a valley, then we assume that the whole valley was affected by that lahar. The valleys can be represented in two ways (Fig. 2b). One way is to draw outlines close to the river courses, which may be most appropriate for mapping the boundaries of lahars. An alternative way is to divide the flanks of the volcano into watersheds. This representation would, for example, allow for the turbulent, upper part of the pyroclastic flows to spread laterally in the valleys. The most appropriate method depends, of course, on the detailed topography of the volcano. In the example using Montagne Pelée, we use present topography which is most relevant to future hazards; however, this may be problematic when mapping past deposits if there have been major changes in topography that need to be taken into account.

Pyroclastic surges

The forces acting on pyroclastic surges are more complex than lahars and pyroclastic flows, because surges are influenced by topography and gravity and also by aerodynamic drag. Surges could be mapped by combining the outline of the river valleys and the Thiessen polygons. Where a surge deposit has been identified, the associated polygon is mapped (i.e. assigned an estimated probability) and, if the site lies in a valley, that part of the valley that is between the site and the vent is also mapped (Fig. 2c).

Laterally directed blasts

It is believed that the wide distribution of laterally directed blasts results from exceptionally high, possibly supersonic, velocities usually directed radially (Crandell et al. 1984). For high-velocity flows, the effects of topography are minor (McEwan and Malin 1989); hence, a mapping technique that takes into account topography is not required. Thiessen polygons are used to map the extent of this type of deposit.

By combining the information contained in the estimated matrix of depositional probabilities derived from the stratigraphy of Montagne Pelée and the simple models defining deposit boundaries, several types of map have been created using a geographical information system (GIS).

Application to Montagne Pelée

Montagne Pelée is composed mainly of pyroclastic deposits produced by three main styles of eruption: Peléean; Plinian; and St. Vincent. The Peléean style involves mainly growth of a lava dome and its partial, repeated collapse under gravity to form a variety of pyroclastic flows. Plinian-style eruptions involve the generation of generally pumiceous deposits from a high eruption column. St. Vincent-style eruptions involve eruption columns of basaltic andesite composition, often producing scoria-and-ash flows (see Smith and Roobol 1990 for more detailed definitions). St. Vincent-style eruptions occurred only at an early stage in the formation of Montagne Pelée, and for the past 14,000 years the eruption style has been either Plinian or Peléean, tending to alternate between the two. However, it is worth bearing in mind that there may be a gradation between the two styles of behaviour, e.g. the largely Peléean eruption of Soufriere Hills Volcano, Montserrat, also produced some pumice flows (e.g. Calder et al. 1999).

Stratigraphic record of Montagne Pelée

There are two main evaluations of the recent stratigraphic record of Montagne Pelée: Westercamp and Traineau

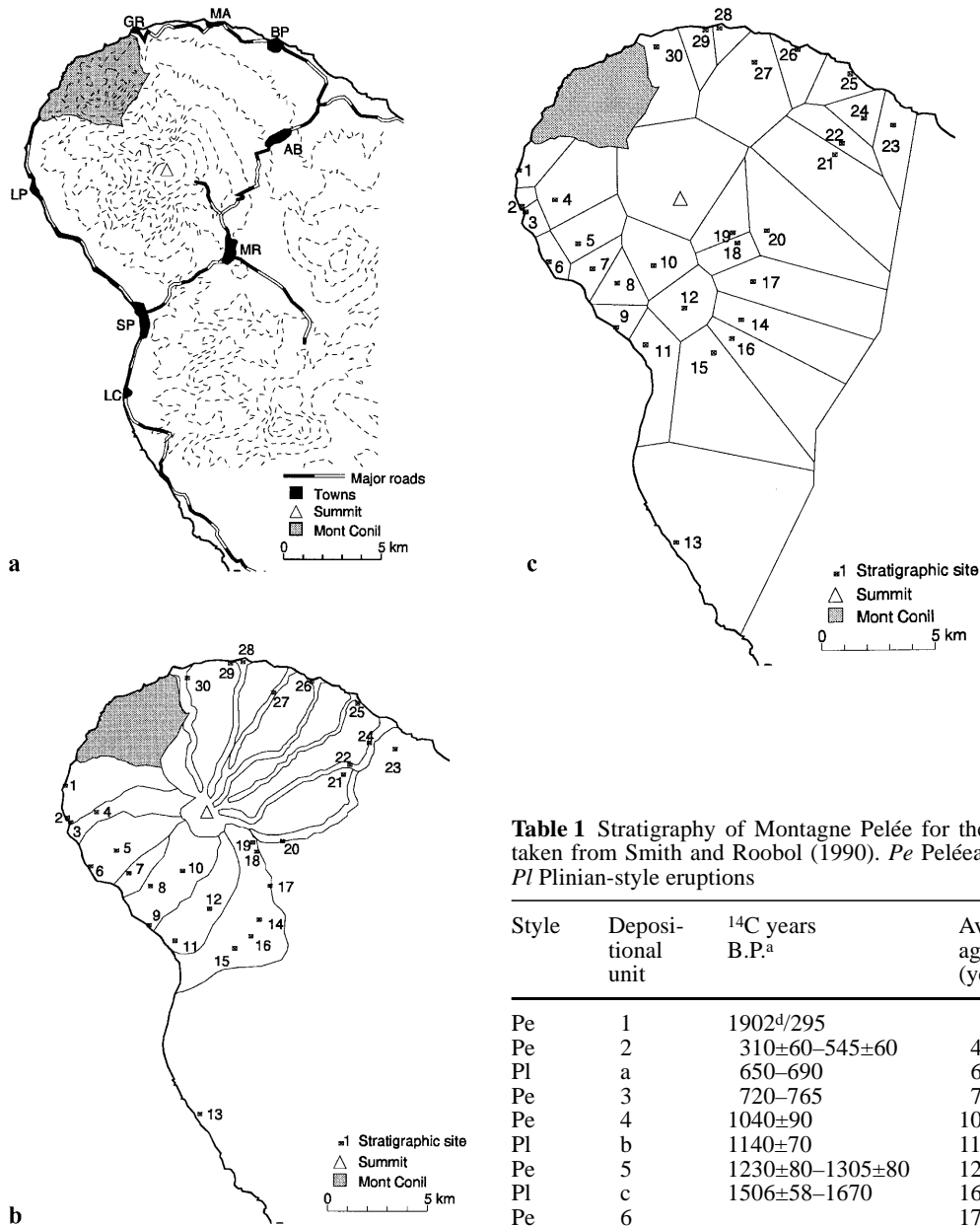


Fig. 3 a Sketch map of the northern part of Martinique showing the contours (500-m interval), main roads and settlements: AB Ajoupa Bouillon; BP Basse Pointe; GR Grand Rivière; LC Le Carbet; LP Le Precheur; MA Macouba; MR Le Morne Rouge; SP St. Pierre. b Combination of the two methods of defining topography most appropriate for Montagne Pelée. Narrow channels that closely follow the course of the major rivers (NE) draining the volcano or the watersheds (SW). c The Thiessen polygon system based on the locations of 30 stratigraphic sites. The vent is treated as a site and therefore a polygon defined by the position of the vent has been generated

(1983); and Smith and Roobol (1990). Herein we largely rely on the latter evaluation. Smith and Roobol (1990) reconstructed the past 14,000 years using 70 deposits, dated using the radiocarbon technique. Their record showed an obvious division in the quality of the record at 6000 years B.P. The majority of ^{14}C ages are less than

Table 1 Stratigraphy of Montagne Pelée for the past 6000 years taken from Smith and Roobol (1990). *Pe* Peléean-style eruptions; *Pl* Plinian-style eruptions

Style	Depositional unit	^{14}C years B.P. ^a	Average age (years) ^b	VEI ^c
Pe	1	1902 ^d /295	45	4
Pe	2	310±60–545±60	430	3
Pl	a	650–690	670	4
Pe	3	720–765	740	3
Pe	4	1040±90	1040	3
Pl	b	1140±70	1140	5
Pe	5	1230±80–1305±80	1270	3
Pl	c	1506±58–1670	1600	5
Pe	6		1730	3
Pl	d	1800±95–2145±70	1940	5
Pe	7	2260±110	2260	3
Pl	e	2390±70–2470±85	2430	5
Pe	8	2490–2750	2600	4
Pe	9	3110±95–3150±65	3130	3
Pe	10	3690–3710	3700	3
Pe	11	3940±80–4005	3980	3
Pl	f	4040–4225±125	4130	5
Pe	12	4300	4300	3
Pl	g	4375±90	4375	4
Pe	13	4410–4560	4500	3
Pl	h	4610–4620	4615	5
Pe	14	4940±105–5240±90	5110	4
Pl	i	5450	5450	5
Pe	15	5650	5650	4
Pl	j	5770±100	5770	4

^a The ^{14}C years are reported relative to a baseline of 1950

^b Average age of ^{14}C ages calculated from data in Fig. 54 of Smith and Roobol (1990)

^c Volcanic explosivity index (Newhall and Self 1982)

^d Actual eruption dates rather than ^{14}C age

Table 2 Definition of deposit terms used in the present study and by Smith and Roobol (1990). *HARI* high aspect ratio ignimbrite; *LARI* low aspect ratio ignimbrite

Eruption style	Eruption process	Deposit terms used in present study	Deposit terms used by Smith and Roobol (1990)
Peléean	Pyroclastic flow Pyroclastic surge	Block-and-ash flow Surge	Block-and-ash flow Dense andesite surge
Plinian	Pyroclastic flow Laterally directed blast Pyroclastic surge	Pumice flow (<i>HARI</i>) Pumice flow (<i>LARI</i>) Pumiceous surge	Pumice-and-ash flow Ash hurricane Pumiceous surge

Table 3 Observed matrix of block-and-ash flow depositional probabilities

Peléean depositional unit	Stratigraphic site											
	3	6	8	9	10	11	12	18	21	22	24	25
1			1	1								
2						1						
3	0.091			1			0.083					
4	0.091		1				0.083					
5	0.182		1		1	0.125	0.083					0.333
6	0.273					0.125	0.083					0.333
7	0.363					0.125	0.083					0.333
8			1			0.125	0.083		1	1	1	
9						0.125	0.083					
10						0.125	0.083					
11			1	1		0.125	0.084					
12				0.02		0.125	0.084					
13		1		0.02			0.084					
14				0.02			0.084					
15				0.02			1	1				
<i>old</i> ^a	7	13	11	11	5	12	15	15	8	8	8	7

^a Contains the depositional unit of the oldest deposit found at each stratigraphic site. The oldest deposit is defined by either a probability of 1 in the cell or by the last depositional unit in a sequence in which the probabilities sum to 1, e.g. as at site 3

6000 years B.P. and the record appears to be comprehensive after this time; thus, we restrict our study to the past 6000 years, as this part of the record is most complete and of uniform quality.

Details of 30 stratigraphic sections have been published and their locations are shown in Fig. 3. There are no sections in the older and largely inaccessible north-west corner of the island (Mont Conil). Several amendments have been made to the stratigraphic data since publication, mainly in response to the authors' queries (A.L. Smith, pers. commun.).

Smith and Roobol (1990) divided the past 6000 years into 25 depositional units (Table 1). These divisions were based mainly on ¹⁴C dates and discontinuities between deposits recognisable in the field. Smith and Roobol (1990) believed these units to be "the closest approximation possible for identifying the products of ancient eruptions"; thus, each depositional unit might represent the deposition from one or more eruptive phases lasting perhaps minutes to days in which a single physical process dominated.

Smith and Roobol (1990) used numbers to identify Peléean eruptions (1–15) and lower-case letters for Plinian eruptions (a–j). The same notation is used in this study. Four main types of deposit (all of essentially an-

desitic composition) have been identified for each style of eruptive behaviour: pyroclastic flow; pyroclastic surge; pyroclastic airfall; and reworked deposits. Table 2 shows how the terms used by Smith and Roobol (1990) for the first two types of deposit are modified in this paper.

Stratigraphic matrices of estimated depositional probabilities

Matrices were constructed for all the different deposits. The majority of deposits have been identified as belonging to a particular depositional unit; therefore, the probability of deposition for these deposits is unity. However, a few deposits are constrained or censored and need to have a probability assigned as previously mentioned. We illustrate this using a block-and-ash flow deposit from a Peléean eruption.

One undated deposit between two dated depositional units

In Table 3, for example, a block-and-ash flow deposit at site 25 has been identified as lying below Plinian unit b

Table 4 The estimates of pd_{ij} , the probabilities of a block-and-ash flow deposit at site i given one at site j

i	j											
Site	3	6	8	9	10	11	12	18	21	22	24	25
3	–	9	0.091	0.045	0.182	0.074	0.200	9	9	9	9	0.273
6	0	–	0	0	0	0	0.092	9	0	0	0	0
8	0.273	9	–	0.667	1	0.200	0.445	9	1	1	1	0.333
9	0.091	9	0.400	–	0	0.067	0.223	9	0	0	0	0
10	0.500	9	0.333	0	–	0.111	0.333	9	9	9	9	1
11	0.102	9	0.075	0.042	0.125	–	0.100	9	0.125	0.125	0.125	0.125
12	0.083	0.084	0.067	0.056	0.083	0.042	–	1	0.083	0.083	0.083	0.083
18	0	0	0	0	0	0	0.500	–	0	0	0	0
21	0	9	0.250	0	0	0.083	0.167	9	–	1	1	0
22	0	9	0.250	0	0	0.083	0.167	9	1	–	1	0
24	0	9	0.250	0	0	0.083	0.167	9	1	1	–	0
25	0.273	9	0.111	0	0.333	0.091	0.200	9	9	9	9	–

Cells containing a “9” indicate where there is “no information” with which to calculate the estimates of pd_{ij}

Table 5 The estimates of pn_{ij} , the probabilities of a block-and-ash flow deposit at site i given that there has been no deposit at site j

i	j											
Site	3	6	8	9	10	11	12	18	21	22	24	25
3	–	0.143	0.182	0.182	0.045	0.160	0.139	0.143	0.143	0.143	0.143	0.121
6	0	–	0	0	0	0	0.076	0.077	0	0	0	0
8	0.455	0.455	–	0.375	0.500	0.507	0.455	0.455	0.429	0.429	0.429	0.444
9	0.318	0.273	0.167	–	0.500	0.315	0.276	0.273	0.286	0.286	0.286	0.333
10	0.176	0.200	0	0.333	–	0.226	0.193	0.200	0.200	0.200	0.200	0.143
11	0.212	0.167	0.250	0.219	0.250	–	0.172	0.167	0.196	0.196	0.196	0.208
12	0.055	0.069	0.069	0.073	0.042	0.075	–	0.071	0.059	0.059	0.059	0.055
18	0	0	0	0	0	0	0	–	0	0	0	0
21	0	0.125	0	0.167	0	0.135	0.122	0.125	–	0	0	0
22	0	0.125	0	0.167	0	0.135	0.122	0.125	0	–	0	0
24	0	0.125	0	0.167	0	0.135	0.122	0.125	0	0	–	0
25	0.121	0.143	0.167	0.200	0	0.156	0.139	0.143	0.143	0.143	0.143	–

and above Plinian unit e (Table 1); therefore, assuming that the deposit belongs to an identified unit, the deposit could belong to Peléean units 5, 6 or 7. Since we do not know to which of these three depositional units it belongs, we assign a probability of a third to each of the three depositional units.

Sequence of undated deposits between dated depositional units

A block-and-ash flow deposit at site 3 is thought to be younger than the 2500 years but has not been attributed to a depositional unit. It is overlain by a Plinian eruption. To calculate the probability that the block-and-ash flow deposit belongs to an identified Peléean depositional unit the order of these two deposits needs to be considered. The Plinian deposit is younger than the Peléean deposit, and so given the dated layers in the stratigraphic record there are 11 different combinations of depositional units to which the deposits could belong: a3; a4; a5; a6; a7; b5; b6; b7; c6; c7; and d7. The probability that the block-and-

ash flow deposit belongs to depositional unit 3 is $1/11=0.091$ and so on for the other depositional units. Other situations involving undated deposits can be dealt with in similar ways. The observed matrix of depositional probabilities for Peléean block-and-ash flow deposits is shown in Table 3. Note the extreme incompleteness of the record (blank cells represent “missing” deposits).

Applying the algorithm

The matrix in Table 3 represents the D matrix and the missing probabilities of deposition are now estimated by applying the algorithm:

1. The first step is to locate the positions of the oldest deposit, old_i , at each site i (the final row in Table 3).
2. The next step is to construct the two probability matrices containing pd_{ij} , the probability of a deposit at site i given one at site j , and pn_{ij} , the probability of a deposit at site i given no deposit at site j using Eqs. (2) and (3), respectively (Tables 4, 5).

Table 6 Estimated matrix of block-and-ash flow depositional probabilities

Peléean depositional unit	Stratigraphic site											
	3	6	8	9	10	11	12	18	21	22	24	25
1	0.106	0.008	1	1	0.197	0.165	0.062	0.003	0.072	0.072	0.072	0.100
2	0.119	0.008	0.440	0.267	0.194	1	0.061	0.003	0.063	0.063	0.063	0.121
3	0.171	0.008	0.488	1	0.173	0.175	0.080	0.004	0.053	0.053	0.053	0.105
4	0.187	0.008	1	0.296	0.245	0.176	0.082	0.004	0.088	0.088	0.088	0.129
5	0.226	0.008	1	0.245	1	0.115	0.087	0.004	0.090	0.090	0.090	0.392
6	0.208	0.008	0.470	0.279	0.243	0.131	0.083	0.004	0.070	0.070	0.070	0.304
7	0.208	0.008	0.470	0.279	0.243	0.131	0.083	0.004	0.070	0.070	0.070	0.304
8	0.127	0.008	1	0.213	0.248	0.110	0.090	0.004	1	1	1	0.131
9	0.132	0.008	0.473	0.289	0.214	0.132	0.082	0.004	0.070	0.070	0.070	0.131
10	0.132	0.008	0.473	0.289	0.214	0.132	0.082	0.004	0.070	0.070	0.070	0.131
11	0.107	0.008	1	1	0.198	0.116	0.081	0.004	0.072	0.072	0.072	0.101
12	0.132	0.008	0.473	0.289	0.214	0.132	0.082	0.004	0.070	0.070	0.070	0.131
13	0.131	1	0.470	0.287	0.213	0.188	0.084	0.004	0.070	0.070	0.070	0.130
14	0.131	0.008	0.470	0.287	0.213	0.188	0.082	0.004	0.070	0.070	0.070	0.130
15	0.141	0.009	0.472	0.280	0.237	0.180	1	1	0.076	0.076	0.076	0.142
Average	0.150	0.074	0.647	0.420	0.270	0.205	0.142	0.070	0.134	0.134	0.134	0.166

3. Cells containing a “9” in Table 4 indicate that the probability estimate could not be calculated because there was not enough information in the matrix. For example, consider sites 3 and 6. The oldest deposit at site 3, old_3 , has been identified as depositional unit 7 and old_6 as depositional unit 13. When comparing two sites, only the information since the youngest depositional unit out of the two oldest deposits are used. This is denoted by l_{ij} . For sites 3 and 6, l_{36} is depositional unit 7. However, there have been no deposits identified at site 6 more recent than depositional unit 7; hence, the denominator in Eq. (2) is zero. Therefore, the probability that there is a deposit at site 3 given one at site 6, pd_{36} , cannot be estimated. This case of “no information” does not matter if pd_{36} is multiplied by d_{t6} in Eq. (4), which equals zero for all t depositional units except unit 13. In this case pd_{36} is omitted from the calculations and the denominator in Eq. (4) decreased accordingly.
4. Once pd_{ij} and pn_{ij} have been calculated, the D_1 matrix can be estimated using Eq. (4) and we continue until convergence. We used a convergence tolerance of 0.001.

The estimated matrix of block-and-ash flow depositional probabilities is shown in Table 6 and the results shown are as expected: the greater the number of deposits that have been identified at a site, and the younger they are, the higher the probability that absent deposits were once present. The mean probability over all depositional units is also calculated and this will be used later.

Defining deposit boundaries

Simple cartographic methods (valley definitions, Thiessen polygons or a combination) are to be used to extend the spatial coverage of the deposition matrix. Herein, we

assume the major elements of topography have not changed in the past 6000 years and use the present topography to define boundaries of past deposits. The valley topography of Montagne Pelée varies across a north-west-to-southeast axis (Fig. 3a). The valleys on the northeast, windward flanks are incised, narrow gorges, separated by areas of gently sloping land. The valleys to the southwest, leeward side of Montagne Pelée have greater relief with high ridges, separating “V-shaped valleys”. Mont Conil, a high massif in the northwest, may act as a barrier to some gravity-driven flows; however, due to the lack of data in this area, it is identified as a separate region.

Two methods of segmenting the topography have been discussed. Valleys were defined by the edges of the gorges in the northeast and by buffers around the valley bottoms in the southwest. The majority of the stratigraphic sites lie in, or close to, river valleys thus defined. The alternative method is to define watersheds. These are clearly defined in the southwest by high ridges that separate valleys, but are less clear in the northeast. Since the topography changes around the volcano, it is more appropriate to combine these two methods so that the drainage channels outline the narrow gorges in the north and east, while the watersheds define the wide valleys in the south and west (Fig. 3b).

The system of Thiessen polygons defined by the location of the stratigraphic sites is shown in Fig. 3c. There is no other information available from locations further afield and so the Thiessen polygons have been bounded by the coastline and a ridge of high land which runs south and east around the volcano and round Mont Conil. The vent is also considered as a “site” and its location taken to be the highest point on the volcano, which is the top of the dome left by the 1929 eruption.

Ideally, the distribution of stratigraphic sites would be dense so that the distances between the sites are small. The greater the distance between sites, the more inaccu-

rate the boundaries are likely to be. Figure 3c shows that the distances between sites are variable and so the Thiessen polygons have very different areas. The polygon associated with site 13 is particularly large, as are those of other sites that extend to the arbitrary eastern boundary.

We now use the deposition probability matrices (fully tabulated in Burt 1995), and spatial boundaries, to create various types of deposit maps. We illustrate them in three applications.

Application I: Individual depositional events

Maps of the spatial distribution of past depositional events are often required and form the basis of preliminary hazard assessments. A depositional event relates to a single row in the stratigraphic matrix. The probabilities in the estimated matrix indicate how likely it was that a deposit now missing was once present. Therefore, a map of a particular depositional event should show not only the areas associated with sites where deposits have definitely been identified (i.e. the probability is unity), but, also, the other sites where the probability of deposition is greater than zero.

The method for mapping all gravity-driven flows is essentially the same, but for the purposes of illustration pyroclastic flows are used. Valleys containing sites where a pyroclastic flow deposit belonging to a particular depositional unit is known to have occurred can be mapped immediately (i.e. assigned a probability of unity). The information from the estimated stratigraphic matrix is used to decide the final position of the deposit boundaries. If more than one site occurs in a valley, the maximum probability associated with the sites are used because, the higher the probability, the more likely it was that the valley had been affected by the deposit, and so we take the worst case when mapping the deposits.

The method for mapping pyroclastic surge deposits involves combining Thiessen polygons and the watersheds. The Thiessen polygons where surge deposits have been identified are mapped and then the valleys between the site and the vent are added. If there is evidence from the complete stratigraphic matrix that other areas may have been affected, then these areas should be mapped in the same way. Depending on the nature of the surge, the polygon surrounding the vent may also need to be mapped.

The boundaries for laterally directed blast deposits are mapped as follows: the Thiessen polygon associated with the vent is mapped first. Other polygons associated with sites where a laterally directed blast deposit has been identified as belonging to a particular depositional period are also mapped. Depending on the location of these positively mapped polygons in relation to the vent, polygons associated with some other sites where there has been no recorded deposit may need to be evaluated. Laterally directed blasts flow over the ground in a direction radial to the vent (Crandell et al. 1984). Lines can be drawn which connect the vent to the sites already

mapped. Any polygon that is crossed by this line is then also assigned the probability of that site. Evidence from the estimated matrix of depositional probabilities that other sites have been affected is then used and polygons associated with these sites are mapped. Again, any polygon crossed by a line between the vent and site, not already mapped, also needs to be considered.

Mapping deposits from the 1902–1903 and 1929–1932 eruptions

It is important to verify the usefulness of any new technique. Detailed maps of the 1902–1903 event have been compiled. Several authors, such as Lacroix (1904), published maps of the effects of the deposits using information collected soon after the event. Since then, various authors have compiled maps based on this previous work (e.g. Smith and Roobol 1990; Tanguy 1994). Figure 4 shows the block-and-ash flow deposits and the lateral extent of the surge deposits which Fisher and Heiken (1982) believed to have destroyed St. Pierre. The 1929–1932 eruption was very similar to the earlier eruption, though on a smaller scale. The later deposits were confined within the envelope of the 1902–1903 deposits and cannot now be properly distinguished from each other (Smith and Roobol 1990); thus, the 1902–1903 deposit map serves for both eruptions and can be used to validate the reconstruction based on stratigraphy.

Our probability map of depositional unit 1 (1902–1903 and 1929–1932 eruptions) is shown in Fig. 5. The areas to have definitely been affected by block-and-ash deposits are similar to those shown in Fig. 4. The model has also predicted additional areas, although the probability of deposition in these areas is 0.5 or less. Overall, the composite probability map of deposits from the 1902–1903 and 1929–1932 eruption generally matches the areas shown in the existing maps of the eruptions but extends beyond them.

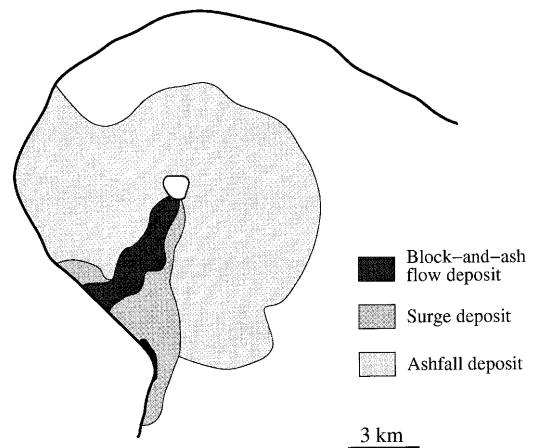


Fig. 4 Map of the 1902–1903 and 1929–1932 eruption products after Smith and Roobol (1990)

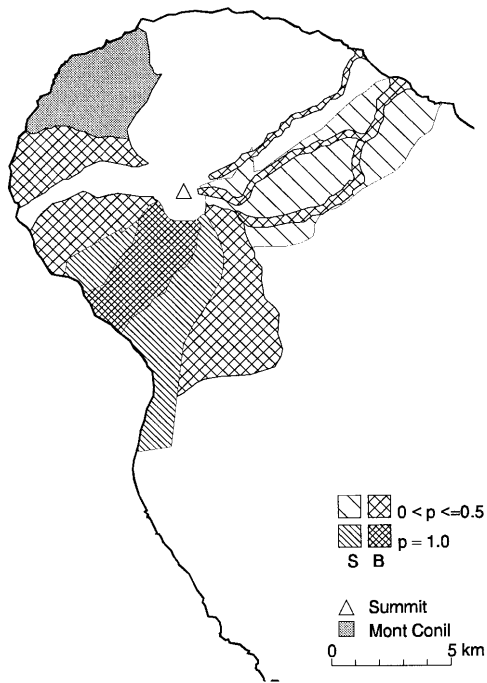


Fig. 5 A map of the probability, p , of distribution of block-and-ash flow (B) and surge (S) deposits

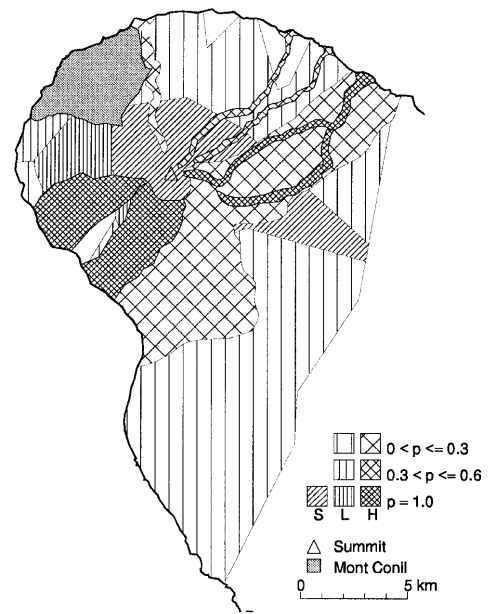
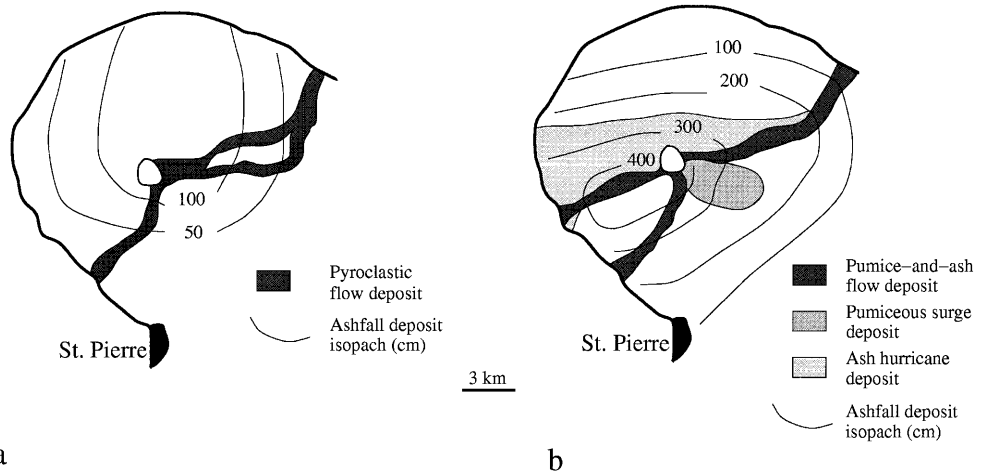


Fig. 7 A map of the composite probability, p , of the distribution of deposits from depositional unit c. The order of plotting is the LAR pumice flow (L) overlain by the pumiceous surge (S), which in turn is overlain by a HAR pumice flow (H)

Fig. 6 Maps of the distribution of deposits from depositional unit c after **a** Traineau et al. (1989) and **b** Smith and Roobol (1990). Thicknesses and isopachs are in centimeters



Mapping deposits from a prehistoric event: depositional unit c

Depositional unit c formed approximately 1600 years ago and produced widespread deposits. Smith and Roobol (1990), and Traineau et al. (1989), have published different maps of the deposits from this event (Fig. 6).

If only the areas associated with sites where deposits have definitely been identified are considered, then the same valleys and the same general areas are indicated on the probability map (Fig. 7) as on the existing maps. However, the probability map indicates that a much larger area could have been affected by laterally directed blasts and more valleys affected by pumice flows, al-

though the probability of these areas being affected is low. The area affected by the pumiceous surge in the probability map is much larger than that shown in Fig. 6b. This is because the Thiessen polygons used to define the area of the surge deposits are large where the distribution of sites is sparse.

Application II: Aggregation by deposit type

The average probability over all depositional units estimates the probability that the site has been affected at some time by that depositional event (final row in Table 6). The map of the average hazard can then be constructed in the same way as for an individual deposition-

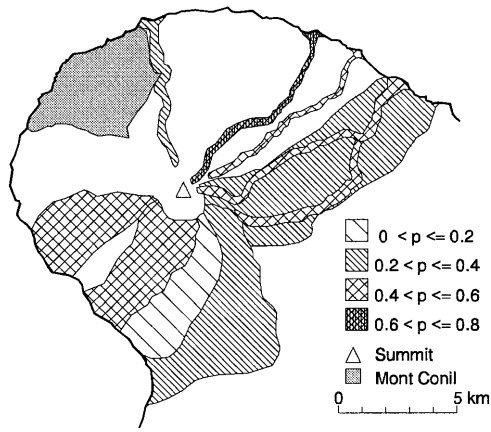


Fig. 8 Map of probability, p , of hazard from pumice-and-ash flows over 6000 years

al event. Figure 8 shows the map of aggregated hazard from high-aspect-ratio (HAR) pumice flows from a Plinian eruption. It shows that the valleys most likely to be affected run southwest and northeast. A watershed has been used in the east because there is depositional evidence that the area relating to site 23, which is outside the narrow channels, has been affected; however, there is a higher probability that the river valley will be affected.

Assuming that activity continues as it has in the past, and that the topography of the volcano does not change, the average probability (written as $p(a_A|e)$, where a_A denotes the occurrence of deposit type A given an eruption e can be used as an estimate of the probability that in any future eruption the site will be affected by that depositional type.

Application III: Eruption scenarios

The probability maps described in the previous section indicate the probability that an area will be affected by a single hazard type during an eruption. However, during an explosive eruption hazards are generated by several processes, as in the 1902–1903 eruption when pyroclastic flows and surges occurred together; therefore, maps combining all possible hazards from an eruption are required. We estimate the probability $p(a|e)$ that an area will be covered by deposits from a future eruption. By combining the probability of average hazard for each deposit type, the probability $p(a|e)$ can be obtained. If an area is likely to be affected only by a single hazard, say hazard A , then $p(a|e)=p(a_A|e)$; however, some areas are likely to be affected by more than one hazard (e.g. A and B), so the probability of these areas being affected is estimated by

$$p(a|e) \approx p(a_A|e) + p(a_B|e). \quad (5)$$

We ignore the joint probability of A and B occurring together to avoid the problem of estimating the probability $p(a_{A+B}|e)$. Moreover, subtracting this probability from

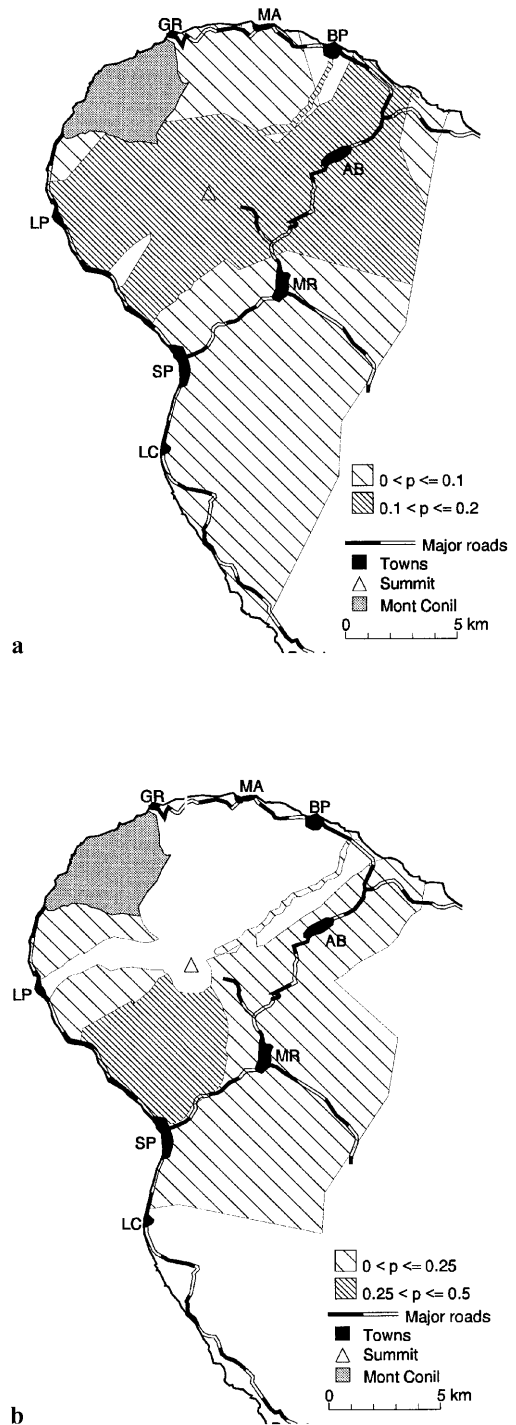


Fig. 9 Scenario map showing the probability, p , of areas being affected over a 100-year period by **a** Plinian eruptions and **b** Peléean eruptions. The settlements around Montagne Pelée are: AB Ajoupa Bouillon; BP Basse Pointe; GR Grand Rivière; LC Le Carbet; LP Le Precheur; MA Macouba; MR Le Morne Rouge; and SP St. Pierre

the right-hand side of Eq. (5) may result in under-estimation.

A more useful and tangible result for planners and civil authorities would be a map displaying the probability $p(a_x)$ of an area being covered during a certain time

period x . The time period chosen needs to reflect the nature of the volcano in question. For Montagne Pelée we use a 100-year period; thus, $p(a_{100})$ can be estimated from

$$p(a_{100})=p(a|e).p(e_{100}), \quad (6)$$

where $p(e_{100})$ is the probability of an eruption in a 100-year period: $p(e_{100})$ is estimated from simple recurrence rates as described in the Appendix.

During a Peléean eruption more than one depositional event occurs generating block-and-ash flow deposits and surge deposits. Similarly, during a Plinian eruption there may be low-aspect-ratio (LAR) pumice flows, HAR pumice flows and pumiceous surges. Therefore, the different hazards from the two eruption styles need to be combined to create Plinian and Peléean hazard maps. The scenario maps in Fig. 9 show that the probability of a Plinian eruption occurring is much lower than for a Peléean eruption, but the area likely to be affected is much greater.

Conclusion

In this paper new methods to map hazards from flow deposits from a stratovolcano, based on the stratigraphic record, are proposed and applied to Montagne Pelée. There are two components to the method; compensating for incompleteness in the stratigraphic record, as far as we are able using the observed stratigraphic record, and using simple mapping techniques to define the extent of deposits. By combining the information in the matrices of estimated depositional probabilities and the definitions of deposit boundaries, three types of map can be created. Maps of past depositional events were constructed by displaying the probability of an individual depositional event. Displaying the mean probability over all depositional events created maps of average probability of deposition over the past 6000 years. Finally, we combined information for several types of deposit and probabilities of deposition to illustrate how these methods could be used as a basis for a more detailed hazard assessment. Two scenario maps were created which displayed the probability deposits from a Plinian and a Peléean eruption occurring in a 100-year period. The usefulness of these maps depends on the assignment of all deposits into one of the two “styles”.

The new methodology has partly compensated for the sampling problems in the stratigraphic record. Also, the mapping techniques have been shown to be simple and adaptable to special cases. We have attempted to quantify the hazard and display this in the probability maps.

The application to Montagne Pelée shows that an objective and generally applicable methodology is possible; however, it does rely on a detailed stratigraphic record, good azimuthal distribution of sample sites and many ^{14}C ages. Currently, few volcanoes have sufficient stratigraphic data of this sort. There is scope for developing the method. The properties of the algorithm devised to

complete the stratigraphic record should be investigated and perhaps improved. Our techniques to map deposit boundaries used only the simplest ideas of geomorphology and physics, and they could be made more realistic. For example, remotely sensed information on the geomorphology and relative age of sectors of the volcano could be used (e.g. Mattioli et al. 1996). More sophisticated mapping techniques based on simulating the physics of the volcanic processes could be combined with this method, e.g. to constrain a Monte Carlo simulation approach.

Acknowledgements We thank A. Smith and H. Traineau for their patience and help with the stratigraphic data. M.L.B. acknowledges support of a NERC postgraduate studentship (ES-/91/PES/3) and G.W.'s work was supported by NERC contract no. F60/G6/12. We also thank C. Newhall, C. Siebe, H. Grubb and T. Druitt for their invaluable comments.

Appendix

Recurrence statistics for Plinian and Peléean eruptions at Pelée

Smith and Roobol (1990) identified 25 depositional units in the past 6000 years. This gives a recurrence rate of one depositional unit every 240 years, and thus the probability of an eruption in the next 100 years $p(e_{100})=0.42$; however, this assumes that the eruption rate is constant over time and does not take into account alternations between Plinian and Peléean eruptions. There have been 10 Plinian depositional units and 15 Peléean depositional units in the past 6000 years; thus, the probability that a Plinian eruption will occur in 100 years is 0.17. For a Peléean eruption the probability is 0.25.

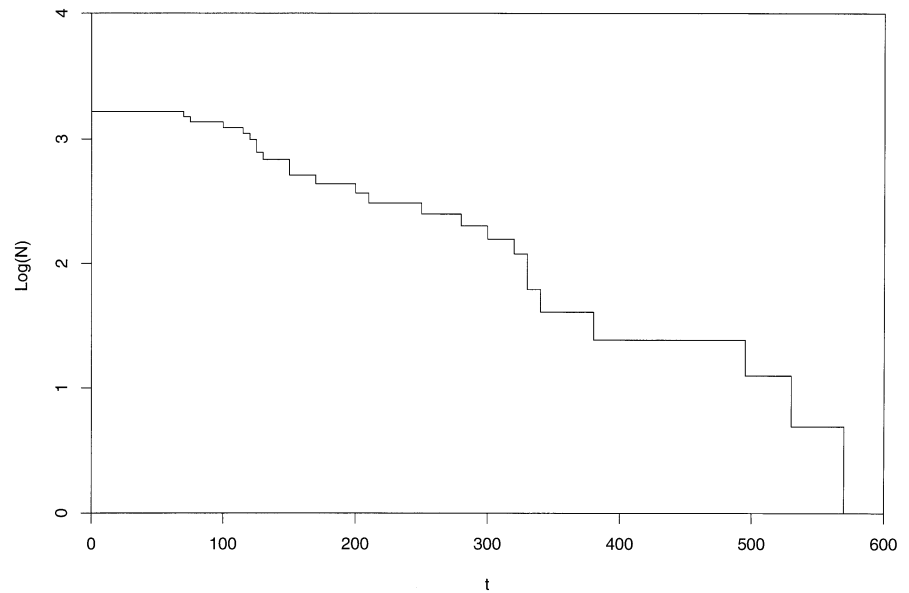
It is likely that all large eruptions in the past 6000 years have been identified, but due to inherent problems with the sampling of deposits this is unlikely to be the case for eruptions of smaller magnitudes. It is unlikely that eruptions of VEI (Newhall and Self 1982) less than 3 will have been identified, or even preserved, in the stratigraphy. The estimates of VEI show that Peléean eruptions are on the whole smaller in magnitude than Plinian eruptions (Table 7). Therefore, the number of Peléean eruptions of small magnitude have been underestimated. To allow for this imbalance in the eruption record, the number of small eruptions needs to be estimated. In a study of volcanic activity in the Lesser Antilles island arc, Smith and Roobol (1990) found that less than half of the historic activity produced deposits likely to be recorded in a stratigraphic study. These deposits were from eruptions of VEI 3 or less. Therefore, simply doubling the number of Peléean eruptions of VEI 3 provides a simple way to allow, albeit arbitrarily, for these unrecorded eruptions. Therefore, the total number of Peléean eruptions in the past 6000 years is now estimated to be 26 and the probability $p(e_{100})$ of Peléean-style is increased to 0.43.

The probabilities $p(e_{100})$ (Fig. 9) are essentially the mean rate of eruption recurrence per 100 years. This implies a constant rate of eruption over time; however, Westercamp and Traineau (1983) suggested that this may not be the case. They attempted to predict the next eruption by using the approach of Wickman (1966). Fig-

Table 7 Volcanic explosivity index (VEI) for eruptions less than 6000 years B.P. at Montagne Pelée

Eruption style	VEI		
	3	4	5
Plinian	0	3	7
Peléean	11	4	0
Both	11	7	7

Fig. 10 A “Wickman-type” diagram of the depositional units of Montagne Pelée, which plots the logarithm of the number of repose periods, N , of duration longer than t years



ure 10 is a “Wickman-type” diagram using the average ages of the depositional units (Table 1) to estimate repose time between eruptions. It shows that an eruption (depositional event) is unlikely to occur within 100 years of the preceding one. After 100 years, the probability of an eruption occurring increases and remains constant up to approximately 350 years. Westercamp and Traineau (1983) related this pattern to the “buffering” effect of the magma chamber. The magma chamber requires a certain amount of time in which to refill to a pre-eruptive state. Therefore, assuming that the 1929 eruption marked the end of the last depositional unit, it appears from the interpretation of Fig. 10 that the next depositional unit is not likely until approximately 2030 A.D. For complex systems, such as Montagne Pelée, the Wickman technique is descriptive rather than quantitative and there is uncertainty in the ^{14}C ages; therefore, we use the probability of an eruption in a 100-year period based on simple recurrence rates of the two types of eruption.

References

- Barberi F, Macedonio G, Pareschi MT, Santacroce R (1990) Mapping the tephra fallout risk: an example from Vesuvius, Italy. *Nature* 344:142–144
- Burt ML (1995) Statistical modelling of volcanic hazards. PhD thesis, Univ Reading, UK
- Calder ES, Cole PD, Dade WB, Druitt TH, Hoblitt RP, Huppert HE, Ritchie L, Sparks RSJ, Young SR (1999) Mobility of pyroclastic flows and surges at the Soufriere Hills Volcano, Monserrat. *Geophys Res Lett* 26:537–540
- Crandell DR, Booth B, Kusumadinata K, Shimozuru D, Walker GPL, Westercamp D (1984) Source-book for volcanic-hazards zonation. UNESCO, Paris, 97 pp
- Druitt TH (1998) Pyroclastic density currents. *Geol Soc Lond Spec Publ* 145:145–182
- Fisher RV, Heiken G (1982) Mt. Pelée, Martinique: May 8 and 20, 1902, pyroclastic flows and surges. *J Volcanol Geotherm Res* 13:339–371
- Harkness DD, Roobol MJ, Smith AL, Stipp JJ, Baker PE (1994) Radiocarbon redating of contaminated samples from a tropical volcano: the Mansion ‘Series’ of St. Kitts, West Indies. *Bull Volcanol* 56:326–334
- Lacroix A (1904) *La Montagne Pelée et ses éruptions*. Masson, Paris
- Mattioli GS, Jansma PE, Jaramillo L, Smith AL (1996) A desktop image processing and photogrammetric method for rapid volcanic hazard mapping: application to air-photo interpretation of Mount Pelée, Martinique. *Bull Volcanol* 58:401–410
- McEwen AS, Malin MC (1989) Dynamics of Mount St. Helens’ 1980 pyroclastic flows, rockslide-avalanche, lahars, and blast. *J Volcanol Geotherm Res* 37:205–231
- Newhall CG, Self S (1982) The volcanic explosivity index (VEI): an estimate of explosive magnitude for historical volcanism. *J Geophys Res* 87:1231–1238
- Okabe A, Boots B, Sugihara K (1992) *Spatial tessellations: concepts and applications of Voronoi diagrams*. Wiley, Chichester
- Rosi M (1996) Quantitative reconstruction of recent volcanic activity: a contribution to forecasting of future eruptions. In: Scarpa R, Tilling RI (eds) *Monitoring and mitigation of volcano hazards*. Springer, Berlin Heidelberg New York, pp 631–674
- Sigurdsson H, Sparks RSJ, Carey SN, Huang TC (1980) Volcanogenic sedimentation in the Lesser Antilles arc. *J Geol* 88: 523–540
- Smith AL, Roobol MJ (1990) Mt. Pelée, Martinique: a study of an active island-arc volcano. *Geol Soc Am Mem* 175:1–105
- Tanguy J-C (1994) The 1902–1905 eruptions of Montagne Pelée, Martinique: anatomy and retrospection. *J Volcanol Geotherm Res* 60:87–107
- Traineau H, Westercamp D, Bardintzeff J-M, Miskovsky J-C (1989) The recent pumice eruptions of Mt. Pelée volcano, Martinique. Part I. Depositional sequences, description of pumiceous deposits. *J Volcanol Geotherm Res* 38:17–33
- Wadge G, Young PAV, McKendrick IJ (1994) Mapping lava flow hazards using computer simulation. *J Geophys Res* 99:489–504
- Westercamp D, Traineau H (1983) The past 5000 years of volcanic activity at Mt Pelée Martinique (F.W.I.): implications for assessment of volcanic hazards. *J Volcanol Geotherm Res* 17:159–185
- Wickman FE (1966) Repose period patterns of volcanoes. I. Volcanic eruptions regarded as random phenomena. *Arkiv Mineral Geol* 4:291–301
- Woods AW (1998) Observations and models of volcanic eruption columns. *Geol Soc Lond Spec Publ* 145:91–114